J Appl Electrochem (2009) 39:2227–2237
DOI 10.1007/s10800-009-9840-3

ORIGINAL PAPER

Influence of calcite on the electrokinetic treatment of a natural clay

Fabio Airoldi · Cristina Jommi · Guido Musso · Elena Paglino

Received: 6 October 2008 / Accepted: 10 February 2009 / Published online: 28 February 2009

Abstract After presenting a geochemical model for the interaction between calcite and varying environmental conditions, the paper discusses the experimental results of long duration electrokinetic tests, run on a natural clayey soil in unbuffered conditions. Local measurements of electrical potential, temperature and water flow were performed during the tests, while pH and fluid conductivity were measured locally once the tests had been dismantled. Sharp change of pH and reduction of the soil electrical conductivity, that in pure clays usually occur in the proximity of the cathode, were observed in the region close to the anode. As well, the soil in the anode area systematically tended to develop fractures, that mostly persisted until the end of the experiments. The features observed, that are not adequately taken into account by existing models, are interpreted in the light of the proposed calcite–water interaction. The onset of fractures, soil desaturation and electrical conductivity drop seem to be justified as a consequence of severe CO_2 pressures arising in the anode area. Calcite dissolution and precipitation is held responsible for the changes of void ratio along the samples.

F. Airoldi · C. Jommi (✉) · E. Paglino
Dipartimento di Ingegneria Strutturale, Politecnico di Milano, Piazza Leonardo da Vinci 32, 20133 Milan, Italy
e-mail: cristina.jommi@polimi.it

F. Airoldi
e-mail: fa.airoldi@tiscali.it

E. Paglino
e-mail: elenapaglino@alice.it

G. Musso
Dipartimento di Ingegneria Strutturale e Geotecnica, Politecnico di Torino, corso Duca degli Abruzzi 24, 10129 Torino, Italy
e-mail: guido.musso@polito.it

Keywords Clayey soils · Electrokinetic treatment · Calcite · Experimental investigation · Geochemical model

List of symbols

$[i]$	Chemical activity of specie i [mol dm^{-3}]
c_i	Concentration of the i-th chemical specie in the water phase [mol dm^{-3}]
D_i	Diffusion coefficient of the i-th chemical specie in free water [m^2 s^{-1}]
e	Void ratio [−]
K_1, K_2	Equilibrium constant for carbonic acid dissociation
K_{calcite}	Equilibrium constant for calcite dissociation
K_{H}	Equilibrium constant for CO_2 dissolution in water
K_{w}	Equilibrium constant for water autoionization
m	Porosity exponent in Archie's formula [−]
M_{c}	Mass of calcite [kg]
M_{i}	Mass of the inert minerals [kg]
n	Porosity [−]
p	Saturation exponent in Archie's formula [−]
p_{CO2}	Pressure of carbon dioxide [atm]
S_{r}	Water saturation [−]
u_i	Ionic mobility of the i-th chemical specie in free water [m^2 V^{-1} s^{-1}]
V_{s}	Volume of the solid phase [dm^3]
V_{v}	Volume of voids [dm^3]
V_{w}	Volume of the water phase [dm^3]
z_i	Charge of the i-th specie
ρ_{i}	Density of the inert minerals [kg dm^{-3}]
ρ_{c}	Density of calcite [kg dm^{-3}]
σ_{w}	Pore water electrical conductivity [S m^{-1}]
σ_{s}	Soil electrical conductivity [S m^{-1}]
S_{s}	Specific surface [m^2 g^{-1}]
w_{L}	Liquid limit [%]

1 Background

The effects of the application of low intensity DC electrical currents to clayey soils have been investigated extensively in the past both for geomechanical and environmental purposes. Several physico-chemical phenomena are recognized to occur simultaneously. Electroosmosis (water flow towards the cathode) and electromigration (flux of charged species towards the oppositely charged electrode) have a relevant practical interest. The first mechanism can be used to induce hydro-mechanical stabilization of the soil mass or the advective transport of non charged contaminants dissolved in the pore water. The second mechanism greatly enhances remediation when contamination is caused by charged species such as heavy metals.

During the process, the imposed electrochemical boundary conditions (electrode reactions, inflow of water with a different chemical composition) and the different mobilities of charged species in water alter significantly the chemical composition of the soil pore water. In unbuffered conditions the electrode reactions lead to the generation of H^+ at the anode and of OH^- at the cathode. Prolonged treatments cause penetration of an acidic front migrating from the anode towards the cathode and of a basic front migrating from the cathode towards the anode. High pH favours the precipitation of heavy metals hydroxides and of salts, so that for remediation purposes enhancement processes have been proposed to control the pH by using acid solutions as catholyte or by introducing cation selective membranes. Since precipitation of chemical species locally reduces the ionic strength of the pore water, the electrical conductivity of the soil is also reduced. Many of these aspects have been satisfactorily taken into account by theoretical and numerical models [1, 2] when reproducing the remediation of pure clays. In this case, the acidic front moves faster than the basic one, so that precipitation and electrical potential drop are usually confined in the soil portion closer to the cathode.

Recently the agreement between simulation results and test data was enhanced by incorporating in the models the effect of pH on several physico-chemical properties of soils. Kim et al. [3] related electroosmotic permeability to the soil pH, Mascia et al. [4] associated a transport model to a geochemical model considering the competitive interaction between cadmium and protons for the adsorption onto the kaolinite surface, while Al-Hadman and Reddy [5] accounted for the reactions occurring in the pore fluid and the surface charge changes induced by pH onto kaolinite minerals surface. Some effects of pH changes on the hydromechanical behaviour of clays have been described in [6].

Previous considerations hold for pure clays, while the investigation of phenomenological behaviour of natural soils still lags behind. Experimental evidences [7, 8] show that if the soil possesses a buffering capacity, for instance due to the presence of carbonates, the acidic front is slowed down, so that alkaline conditions dominate over a wider part of the soil mass. A dramatic drop in electrical conductivity occurs at the anode side, instead of at the cathode side. Consequences of calcite dissolution and precipitation during electrokinetic treatments on the mechanical behaviour of the soil have been documented as well [9]. High pH environment and concomitant precipitation of carbonates promote a cementation effect, which increases the soil stiffness and may be lost under mechanical destructuration.

In the present work a simple geochemical model for calcite dissolution and precipitation is presented, and its implication in terms of CO_2 pressure, water saturation and changes of void ratio are discussed. The model predictions are compared with experimental data coming from unbuffered electrokinetic tests performed on a natural moderately carbonatic clay.

2 Soil properties and experimental conditions

Unbuffered electrokinetic tests were run on remoulded samples of Scanzano Clay. This is a natural illitic-kaolinitic strongly structured scaly clay, with a small quantity of smectite. The soil physical parameters were determined following standard testing procedures [10–12]. The soil has a liquid limit $w_L = 58\%$, a plasticity index $PI = 0.30$ and an activity (the ratio between the plasticity index and the percentage of particles with an equivalent diameter smaller that 2 μm) equal to $A = 0.88$. Its natural carbonate content, expressed as the ratio between the equivalent weight of calcite and the weight of the solid grains, ranges around 15%. The carbonate content of the soil studied is comparable to that of many common natural soils.

Samples were prepared starting from ground air dried material. The soil powder was mixed with a 10^{-2} M KCl solution in distilled water to a water content of about 1.5 times the liquid limit to achieve water saturation, and left to homogenise for 24 h. The composition of the pore fluid was chosen to ensure stability of the silver probes adopted to measure locally the electrical potential drop and its variations during the test. The slurry was then poured in a cylinder with rigid lateral walls and one dimensionally consolidated in load steps up to a vertical stress of 100 kPa. After preparation, the saturated samples had a void ratio of about $e_0 = 0.95$, corresponding to a water content $w_0 = 0.347$. At w_0 conditions, the pore water of the sample had an electrical conductivity $\sigma_w = 0.98$ S m^{-1}, that would correspond to an equivalent KCl concentration of $9.8 \cdot 10^{-2}$ M. The difference between the conductivity of the solution used to saturate the soil samples and the one

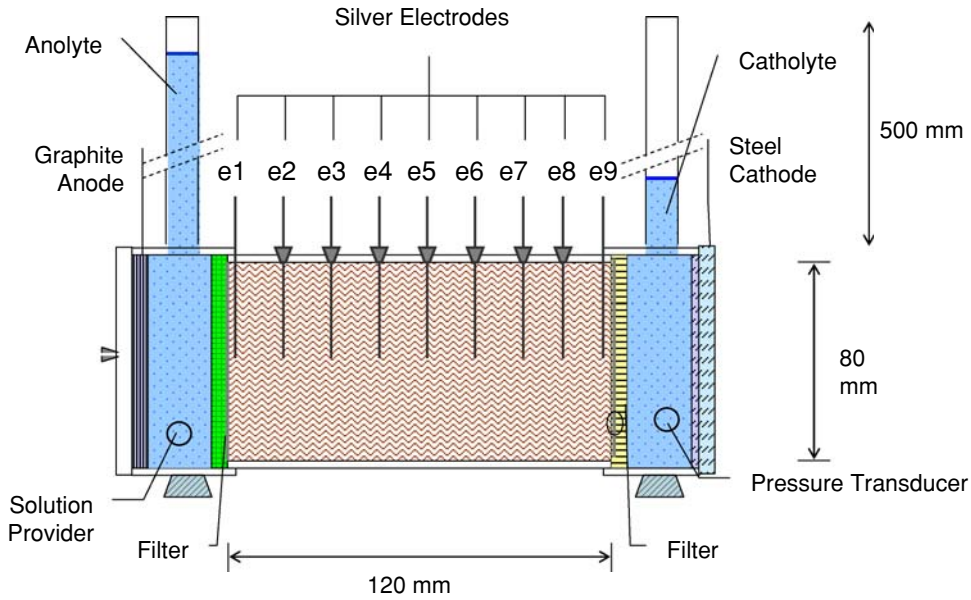

Fig. 1 Scheme of the electrokinetic filtration cell

measured is due to the presence of the salts originally present in the soil dissolved by saturation, whose nature was not investigated.

The samples were then extracted and mounted in the experimental cell for testing. The experimental cell used is sketched in Fig. 1. Electrical current is injected into cylindrical soil samples (80 mm in diameter, 120 mm in length) by a graphite anode and a steel cathode. An anolyte and a catholyte reservoirs separate the soil sample from the electrodes, allowing the gas produced by electrode reactions to leave the cell without entering the soil. Other details concerning the experimental cell can be found in [13]. A 10^{-2} M KCl solution in distilled water, identical to that used for the preparation of the samples was circulated from the anode during the entire duration of the tests presented. The electrical potential drop over the soil mass was monitored continuously by means of nine silver electrodes, equally spaced over the soil sample, while five thermocouples are placed to monitor temperature variations.

3 Geochemical model

3.1 Equilibrium reactions

The geochemical system proposed [14] considers the mutual interactions that the three phases constituting the soil (solid, gas and water) must satisfy in the presence of calcite and evolving chemical conditions.

The solid phase of Scanzano clay is constituted by clay minerals and calcite ($CaCO_3$). Depending on their crystalline structure, clay minerals can exhibit a certain buffering capacity, related to their specific surface, S_s, and Cation Exchange Capacity CEC. The specific surface of Scanzano clay has been evaluated to range around 70 $m^2\ g^{-1}$ according to the relationship quoted by [15]:

$$S_s = 1.8 w_L - 34 \quad (1)$$

On the basis of the specific surface and mineralogy, a CEC of about 15 m^2/100 g is expected [16]. Given the moderate CEC, as a first assumption, the clay minerals have been considered inert in the study of the electro-hydro-mechanical behaviour of the soil, while the chemical behaviour of the calcite has been explicitly taken into account.

The gas phase could be considered as a mixture of different gases, with carbon dioxide being the only one allowed to take part to the chemical reactions.

As for the water phase, the initial water electrical conductivity reported in the previous section ($\sigma_w = 0.98$ S m^{-1}) suggests the presence of several indigenous ionic species. However, the only species considered in the geochemical model are H^+, Ca^{2+}, OH^-, HCO_3^-, CO_3^{2-} and $H_2CO_3^*$, since those are the ones that participate to the equilibrium of the calcite system, while other species possibly present such as Mg^{2+} and Na^+ do not interfere with it. The notation $H_2CO_3^*$ represents the sum of the carbon dioxide dissolved in water and of carbonic acid:

$$H_2CO_3^* = CO_{2(aq)} + H_2CO_3. \quad (2)$$

The geo-chemical model summarises the primary reactions governing the evolution of the three-phase system. Two of the reactions imply exchange of mass

between the different phases. The first one governs the dissolution/precipitation of calcite:

$$\mathrm{CaCO_3} \leftrightarrow \mathrm{Ca^{2+}} + \mathrm{CO_3^{2-}} \quad \left(K_{\mathrm{Calcite}} = \left[\mathrm{Ca^{2+}}\right]\left[\mathrm{CO_3^{2-}}\right] \cong 10^{-8.3}\right), \tag{3}$$

whereas CO_2 is interchanged between the gas phase and the water phase depending on its pressure:

$$\mathrm{CO_{2(g)}} + \mathrm{H_2O} \leftrightarrow \mathrm{H_2CO_3^*} \quad \left(K_{\mathrm{H}} = [\mathrm{H_2CO_3^*}]/p_{\mathrm{CO_2}} \cong 10^{-1.5}\right). \tag{4}$$

All the other reactions take place only in the water phase and are related to the dissociation of carbonic acid and to water ionization:

$$\mathrm{H_2CO_3^*} \leftrightarrow \mathrm{H^+} + \mathrm{HCO_3^-} \quad \left(K_1 = [\mathrm{H^+}][\mathrm{HCO_3^-}]/[\mathrm{H_2CO_3^*}] \cong 10^{-6.3}\right) \tag{5}$$

$$\mathrm{HCO_3^-} \leftrightarrow \mathrm{H^+} + \mathrm{CO_3^{2-}} \quad \left(K_2 = \left[\mathrm{H^+}\right]\left[\mathrm{CO_3^{2-}}\right]/[\mathrm{HCO_3^-}] \cong 10^{-10.3}\right) \tag{6}$$

$$\mathrm{H_2O} \leftrightarrow \mathrm{H^+} + \mathrm{OH^-} \quad \left(K_{\mathrm{w}} = [\mathrm{H^+}][\mathrm{OH^-}] \cong 10^{-14}\right) \tag{7}$$

Equilibria of the carbonatic species in water given by (4) and (5), associated to the equilibrium of CO_2 in water (3) and the water auto ionization equilibrium (6), imply a direct relationship between the CO_2 pressure and the acidity of the water solution. Increasingly higher CO_2 pressures are needed to lower pH, and basic conditions correspond to modest CO_2 pressures.

Finally, electroneutrality of the water phase introduces a further constraint on the system:

$$2c_{\mathrm{Ca^{2+}}} + c_{\mathrm{H^+}} = c_{\mathrm{HCO_3^-}} + 2c_{\mathrm{CO_3^{2-}}} + c_{\mathrm{OH^-}}. \tag{8}$$

The geochemical system is defined by eight unknowns, mass of calcite, mass of the six dissolved species and CO_2 pressure, and it is constrained by the six equations (2)–(7). The number of unknowns can be reduced to seven by noting that, since calcite belongs to the solid phase, its actual amount does not intervene in any of the equilibrium constants. Hence, one further condition is necessary to quantify the mass of species dissolved in water and CO_2 pressure. The common practice in geochemical analysis is to impose the seventh condition in terms of the constraint imposed to the system by the local surrounding environment, as, for example, constant CO_2 pressure in a so-called *open system* or no mass exchange in a *closed system.* Actually, in the tests that will be presented in the following, the local constraints can not be controlled directly and they may change throughout the tests. Hence, a different viewpoint, that will be discussed in Sect. 5, was chosen, in order to compare the model predictions with experimental data at the end of the tests run.

3.2 Relationship between phases

Since the reactions considered involve all the three phases constituting the soil and affect the mass of their chemical constituents, their occurrence will necessarily alter the volume fractions of the soil phases. The actual mass of solid calcite and of CO_2 gas is given by the sum of their initial values and of the mass produced or consumed due to the time evolution of reactions (3) and (4), and the volume of the two constituents will evolve consequently.

As customary in soil mechanics, the relationships between the volumes of the different phases can be expressed in terms of void ratio,

$$e = \frac{V_{\mathrm{v}}}{V_{\mathrm{s}}} = \frac{V_{\mathrm{v}}}{\frac{M_{\mathrm{i}}}{\rho_{\mathrm{i}}} + \frac{M_{\mathrm{c}}}{\rho_{\mathrm{c}}}}, \tag{9}$$

and degree of water saturation,

$$S_{\mathrm{r}} = \frac{V_{\mathrm{w}}}{V_{\mathrm{v}}}. \tag{10}$$

In the expressions (9) and (10), V_{v} is the volume occupied by voids, V_{w} is the water volume, and V_{s} is the total solid volume. Accordingly to the hypothesis introduced previously, the latter may be considered as the sum of the constant volume occupied by inert clay (subscript i) and the variable volume occupied by reactive calcite grains (subscript c). In the right hand side of expression (9) the latter are written in terms of mass and density of the two species.

Assuming negligible overall volumetric deformation, it is straightforward to account for the effect of precipitation or dissolution of calcite, since in this case the variation of the volume of voids is equal and opposite to the variation of the volume of the solid phase. If ΔM_{c} is the calcite mass variation, the actualised void ratio, $e^{(1)}$ reads:

$$e^{(1)} = \frac{V_{\mathrm{v}}^{(0)} - \frac{\Delta M_{\mathrm{c}}}{\rho_{\mathrm{c}}}}{\frac{M_{\mathrm{i}}}{\rho_{\mathrm{i}}} + \frac{(M_{\mathrm{c}} + \Delta M_{\mathrm{c}})}{\rho_{\mathrm{c}}}}. \tag{11}$$

In principle, changes of the water saturation degree could be calculated as well, knowing the variation of void volume caused by reaction (3) and the mass of gaseous CO_2 released. Still, the latter is uniquely determined only in terms of the constraint imposed to the system by the local hydraulic conditions. If gas can escape from the soil or its transport rate is high, CO_2 pressure will rapidly decrease, while higher pressures may develop if CO_2 remains entrapped locally into the soil void structure. As already observed in the previous section, in the tests performed local hydraulic constraints change during the test and are not directly controlled. For this reason, a relationship between degree of water saturation and CO_2

pressure at equilibrium, based on the capillary retention properties of the soil has been introduced here. Disregarding water pressure changes with respect to those of the gas phase, capillary pressure may be identified with the difference between CO_2 pressure imposed by the geochemical reactions and the initial water pressure. Capillary pressure curves can then be used at this stage to derive the theoretical degree of saturation associated to a given CO_2 pressure.

4 Experimental evidence

Four tests, at controlled constant electrical current $I = 40$ mA (equivalent to a current density $i = 0.8$ mA cm^{-2}), were run. Tests lasted 14 days, allowing for about an entire pore volume of water to filtrate through the samples. At the end of the tests the samples were dismantled and cut into four slices, 3 cm thick each, for subsequent characterisation. Table 1 provides a list of the quantities measured at the end of each test.

Time evolution of potential drop in the Casp_er_01 test is represented in Figs. 2 and 3. Potentials are referred to the last (cathode side) silver measurement electrode. In Fig. 2 single electrodes measurements are reported as a function of time, while in Fig. 3 isochrones of the potential drop along the sample are represented. During the first 130 h, the electrical field remains almost homogeneous along the sample, although it increases as a consequence of the ionic depletion occurring in the soil water because of species transport towards the electrodes. The potential drop between the first and the second electrode has then a sharp increase that, at controlled constant electrical current, is related to a marked local decrease of the soil electrical conductivity. The same sharp increase can be observed in the other tests (after 120 h in the CBC sample, and after 124 and 130 h in the Casp_er_02 and Casp_er_03 samples, respectively). After about 300 h the decrease of the electrical conductivity begins to move further inside the sample, as the third electrode measurement shows. The same phenomenon occurs in the other tests after 315, 260 and 300 h, respectively.

Increase in electrical resistivity at the anode end was accompanied in all cases by the onset of evident fractures in the soil mass, most of them persisting until the end of the test. Figure 4 documents open fractures at test dismantling for samples CBC and Casp_er_02.

Soil pH, shown in Fig. 5, was distributed highly non-linearly inside the samples, being very low in the proximity of the anode, but rapidly increasing already at limited distance. The pH measurements performed after the tests were reproducible, the scatter being within a pH unit. Only the first fourth of the samples developed acidic conditions, while in the rest of the samples basic conditions prevailed. Accordingly, dissolution of carbonates is documented to have occurred quite extensively in the first three centimetres, while precipitation occurred in the remaining part of the samples, as Fig. 6 shows. Differences in the carbonate mass variations between the samples at given points were below 1%.

5 Comparison between experimental measurements and model predicitons

Available models calibrated on pure clays satisfactorily reproduce the chemical conditions developing in soil samples after extended treatment times, comparable to those of the present study. Both models and experiments conducted on pure clays foresee dramatic changes in pH distribution inside the soil, but with a wider portion on the anode side evolving towards extremely acid conditions and a smaller portion on the cathode side evolving towards definitely basic conditions. The evidence is explained by a higher mobility of the protons generated by the electrochemical reactions at the anode. During remediation of soils contaminated by heavy metals, this is a positive outcome of the technique, since H^+ is able to replace the contaminants

Table 1 Synopsis of the tests run on the treated samples

	CBC	Casp_er_01	Casp_er_02	Casp_er_03
Specific weight		•		
Liquid limit w_L	•	•		
Plastic limit w_P	•	•		
Water content w	•	•		
Saturation degree S_r	•	•		
pH	•	•	•	•
Carbonate content	•	•		
One dimensional compression tests	•			
Electrical conductivity and pH of the pore fluid		•		
Electrical conductivity and pH of the reservoirs	•	•	•	•

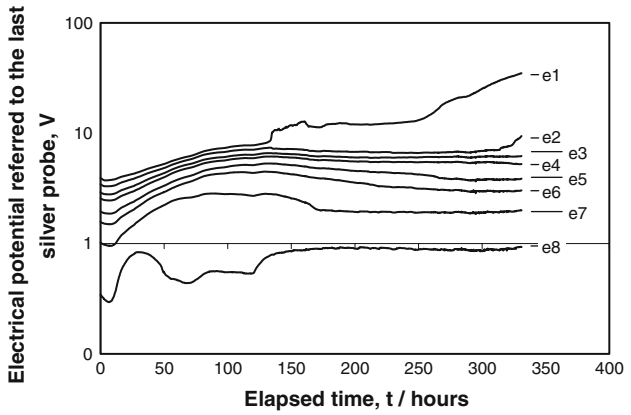

Fig. 2 Test Casp_er_01: time evolution of electrical potential V measured inside the sample. Reference value is the voltage read by electrode $e9$ in Fig. 1

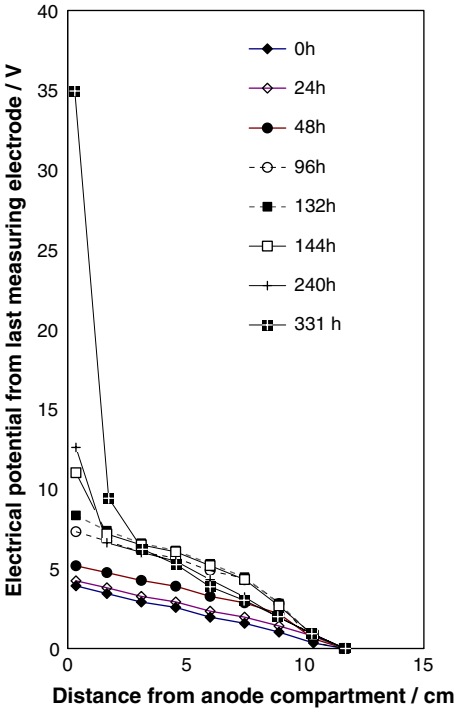

Fig. 3 Test Casp_er_01: isochrones of electrical potential distribution. Reference is the voltage read by electrode $e9$

adsorbed on clay particle surfaces and promote their migration towards the cathode. As well, basic conditions at the cathode side favour the precipitation of salts and hydroxides, locally reducing the concentration of ions in the pore fluid and the associated electrical conductivity. As a final consequence, the electrical potential drop in the treated soil mass is moderate at the anode side, while significant potential gradients develop at the cathode side.

The experimental results of this study, discussed in the previous section, qualitatively differ from most literature observations. Still, the chemical conditions characterising pure systems, and the associated transport and mechanical properties, can change greatly if buffering species, such as carbonates, are present. The model presented in Sect. 3 was exploited to verify the relevance of the buffering capacity of calcite in the context of the present study, under the hypothesis that the kinetics of the reactions are sufficiently fast to ensure chemical equilibrium.

The concentrations of the chemical species of the calcite-CO_2 system were calculated with reference to the end of the tests. The predicted final volume fractions in terms of void ratio and saturation degree were then compared to measured values. Comparison was made as well between the theoretical electrical conductivity of the ionic species of the geochemical model (global value) and the measured electrical conductivity.

To definitely close the geochemical model, a further condition had to be imposed. Equilibrium of the considered chemical species is related to the CO_2 pressure, which is a variable of the problem as well. In principle, the pressure could be evaluated by considering locally the CO_2 mass balance, by taking into account explicitly the transport of the various chemical species. Nevertheless this approach poses serious problems, since a critical point is the transport of the gaseous CO_2 developed by the chemical reactions. Transport of the gaseous phase was documented by the developed fractures and by gas escaping from the boundaries of the soil samples observed during the tests. Explicit assumptions on the hydromechanical conditions leading to fractures and subsequent gas flow should be introduced, an aspect that deserves further investigations.

However, the geochemical system at a given time is determined if the concentration of a single species is known. As pH was measured in a few sections of the sample at the end of the test, its values were thus used to provide the missing constraint condition needed to determine the local activities of the other chemical species of interest and the associated CO_2 pressure. For the Casp_er_01 sample, the procedure leads to the expected activities and pressures collected in Table 2.

Figure 7 compares the void ratios measured at the end of the test with those predicted by using Eq. 10. The qualitative trend predicted by the model is good, and the quantitative predictions are satisfactory, with moderate errors (below 10%) at the anode side for the Casp_er_01 sample. Different causes can be claimed to be responsible of the scatter observed, among them the most likely being local changes of water pressure [17]. Indeed, the cell arrangement dictates a uniform liquid flow rate. The transition from low to high electrical gradients, occurring in the first centimetres of the sample, would cause net water accumulation, unless an opposing Darcian flow arose, that in turn requires a local increase in water pressure. Increasing water pressure implies a decrease of the effective

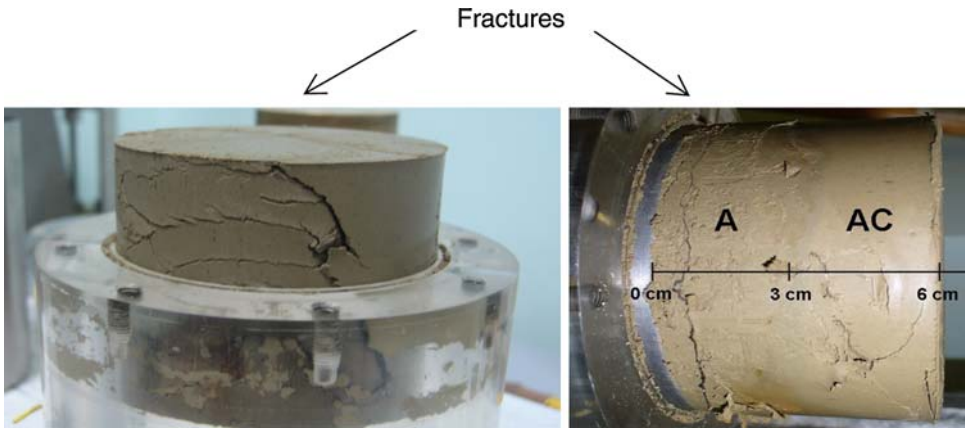

Fig. 4 Fractures detected at tests dismantling in the anode side. Tests CBC (*left*) and Casp_er_02 (*right*)

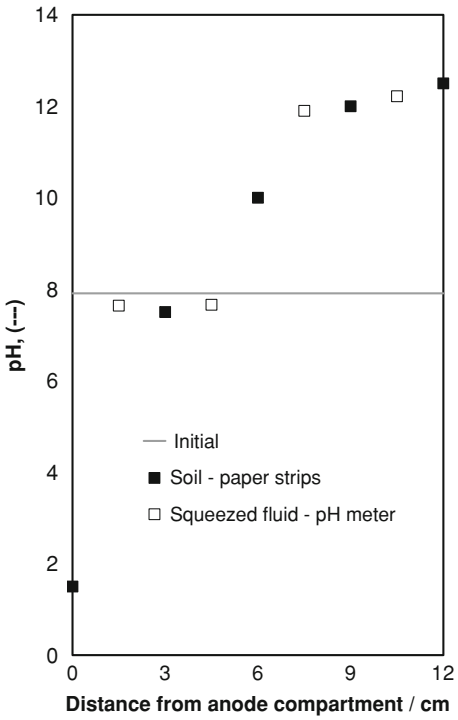

Fig. 5 Casp_er_01 test: pH distribution before and after electrokinetic filtration

mechanical stress acting on the soil skeleton, producing soil swelling, i.e. a net increase in the local void ratio. This mechanism was not included in the model, since it only considers void ratio changes due to dissolution of calcite.

The typical water saturation profile at the end of the tests is reported in Fig. 8. The data show a partial desaturation of the part of the sample close to the anode, while the rest of the sample, where basic conditions prevail, remains saturated. The soil treated possesses a relatively high resistance to gas penetration, and high gas pressures are needed to lower the water saturation degree to the values observed. It is well known that gas begins to flow through the porous matrix once it has reached the breakthrough pressure forcing it into the specimen. Gas breakthrough is frequently accompanied by a marked peak of gas pressure that decreases afterwards. This behaviour is explained by assuming that, after penetrating into the solid matrix, gas flows through preferential paths developed by the initial gas pressure peak via an hydraulic fracturing mechanism [18].

The latter interpretation may serve in explaining the role played by the high CO_2 pressures expected to develop in acidic environment. As pH lowers, CO_2 pressure increases up to a peak value sufficient to reach the breakthrough pressure and to initiate the hydraulic fracturing mechanism. The gas pressure then lowers, while the gas front advances into the soil matrix. The theoretical final CO_2 pressures in equilibrium with the measured degrees of water saturation can be derived from Fig. 9a, where the capillary pressure curve of the soil at the void ratio of interest is given [19, 20]. A degree of water saturation of 0.87 can be maintained with a gas pressure of about 10 atm, in equilibrium with a calculated pH value in the range between 5 and 6 (see Fig. 9b). The theoretical pH value is consistent with the pH trend observed experimentally. It's worth noting that, in principle, more severe pressures, that are consistent with the lower pH values recorded in the anodic side, are needed to initiate soil fracturing, that in fact was systematically observed in the first part of the sample, close to the anode.

The ionic concentrations calculated with the model, assumed to be equal to the respective activities of Table 2, were used to derive theoretical electrical conductivity values, estimated by applying the Nernst–Einstein equation to derive the ionic mobility of each species in solution:

$$u_i = \frac{D_i z_i F}{RT}, \tag{12}$$

and then by summing up the contributions of all species:

$$\sigma_w = F\left(\sum_{i=1}^{n} c_i z_i u_i\right) = F^2\left(\sum_{i=1}^{n} \frac{c_i z_i^2 D_i}{RT}\right). \tag{13}$$

Predicted electrical conductivities are compared with the ones measured on the pore fluid squeezed from the

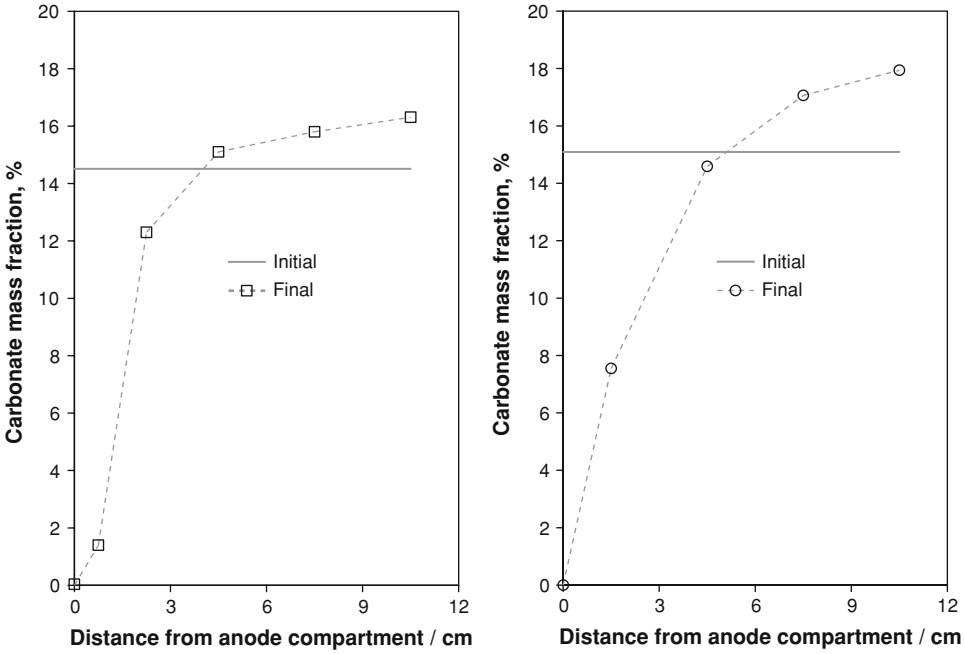

Fig. 6 Initial and final carbonate distribution in the samples Casp_er_01 (*left*) and CBC (*right*)

Table 2 Casp_er_01 test: activities of the species modelled and CO_2 pressure predicted by the geochemical model

	Initial conditions	Distance from anode compartment/cm					
		0*	1.5	4.5	7.5	10.5	12
pH	7.91	1.54	7.64	7.66	11.9	12.22	12.57
$[H^+]$	$1.23 \cdot 10^{-8}$	$2.88 \cdot 10^{-2}$	$2.29 \cdot 10^{-8}$	$2.19 \cdot 10^{-8}$	$1.26 \cdot 10^{-12}$	$6.03 \cdot 10^{-13}$	$2.69 \cdot 10^{-13}$
$[OH^-]$	$8.13 \cdot 10^{-7}$	$3.47 \cdot 10^{-13}$	$4.37 \cdot 10^{-7}$	$4.57 \cdot 10^{-7}$	$7.94 \cdot 10^{-3}$	$1.66 \cdot 10^{-2}$	$3.72 \cdot 10^{-2}$
$[CO_3^{2-}]$	$6.38 \cdot 10^{-6}$	$1.40 \cdot 10^{-2}$	$4.68 \cdot 10^{-6}$	$4.79 \cdot 10^{-6}$	$1.26 \cdot 10^{-6}$	$6.04 \cdot 10^{-7}$	$2.70 \cdot 10^{-7}$
$[HCO^{3-}]$	$1.57 \cdot 10^{-3}$	$8.32 \cdot 10^{-4}$	$2.14 \cdot 10^{-3}$	$2.09 \cdot 10^{-3}$	$3.17 \cdot 10^{-8}$	$7.26 \cdot 10^{-9}$	$1.45 \cdot 10^{-9}$
$[Ca^{2+}]$	$7.86 \cdot 10^{-4}$	–	$1.07 \cdot 10^{-3}$	$1.05 \cdot 10^{-3}$	$3.97 \cdot 10^{-3}$	$8.30 \cdot 10^{-3}$	$1.86 \cdot 10^{-2}$
$[H_2CO_3^*]$	$3.84 \cdot 10^{-5}$	$4.79 \cdot 10^{1}$	$9.77 \cdot 10^{-5}$	$9.12 \cdot 10^{-5}$	$7.96 \cdot 10^{-14}$	$8.73 \cdot 10^{-15}$	$7.78 \cdot 10^{-16}$
p_{CO2} [atm]	$1.21 \cdot 10^{-3}$	$1.51 \cdot 10^{3}$	$3.09 \cdot 10^{-3}$	$2.88 \cdot 10^{-3}$	$2.52 \cdot 10^{-12}$	$2.76 \cdot 10^{-13}$	$2.46 \cdot 10^{-14}$

*Values refer to a theoretical system without calcite, where equilibrium reactions are $CO_{2(g)} + H_2O \leftrightarrow H_2CO_3^*$, $H_2CO_3^* \leftrightarrow H^+ + HCO_3^-$, $HCO_3^- \leftrightarrow H^+ + CO_3^{2-}$, $H_2O \leftrightarrow H^+ + OH^-$

samples [21] after the end of the tests in Fig. 10. As in the geochemical model only the species that are reactive with respect to the calcite system are considered, the theoretical electrical conductivities do not include the possible contribution of other ions. Consistently, theoretical electrical conductivities calculated by the model are lower than the measured ones. It is interesting to notice, however, that the difference between predicted and measured values is moderate and that for the section at 1.5 cm it ranges around 0.1 S m^{-1}, comparable to the one of the 10^{-2} M KCl solution fed at the anolyte compartment (0.14 S m^{-1}).

The geochemical system could help as well in explaining the observed decrease of electrical conductivity close to the anode. On the one hand, pH value justifies chemical equilibria that locally reduce the ionic strength and therefore the electrical conductivity of the fluid. On the other hand, decrease of saturation accompanying gaseous CO_2 development, reduces the water transmissivity of the porous medium lowering the electromigrative transport of the dissolved ions, the gas phase being electrically non conductive.

The impact of desaturation on electrical conductivity of the soil studied can be appreciated with reference to Fig. 11, where the potential drop measurements at the final stage of test Casp_er_01 are compared with synthetic ones obtained assigning to the four sample portions characteristic average electrical conductivity values. The latter were estimated by neglecting the contribution of surface electrical conductivity and adopting Archie's formula [22]:

$$\sigma_s = n^m S_r^p \sigma_w. \quad (14)$$

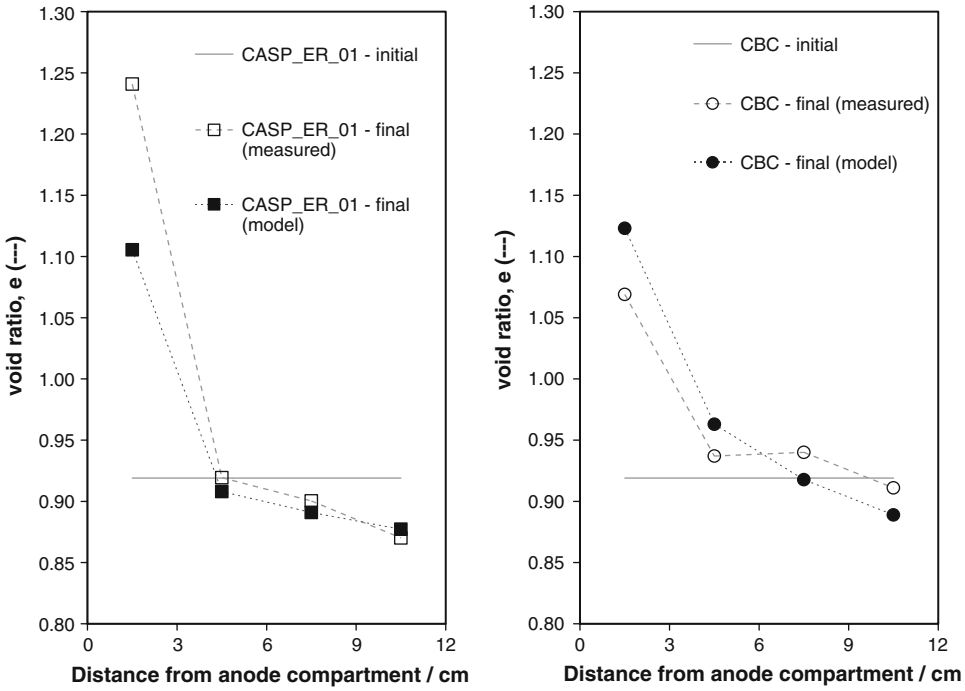

Fig. 7 Measured (*empty*) and calculated (*full*) void ratios upon test dismantling of two electrokinetic filtration tests run under the same conditions

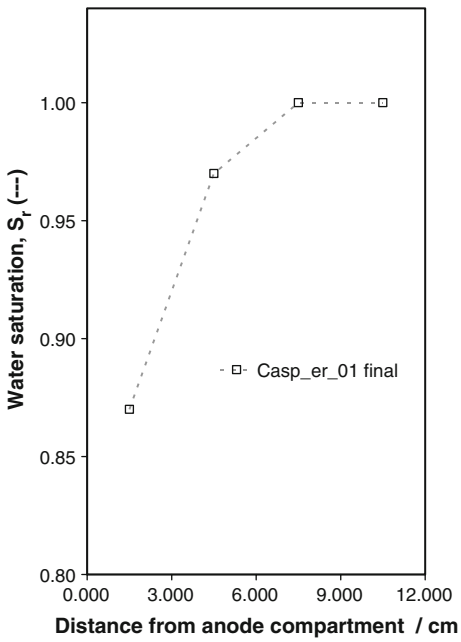

Fig. 8 Water saturation along the sample Casp_er_01 at test dismantling

A value of 1.91 was adopted for the empirical factor *m*, accounting for the effect of tortuosity on the electromigration process in a porous medium, on the basis of the initial electrical conductivity of the soil and of its pore water. The exponent *p*, that reflects the impact of water saturation degrees lower than one, was assumed equal to 2.4 on the basis of literature considerations [16]. The

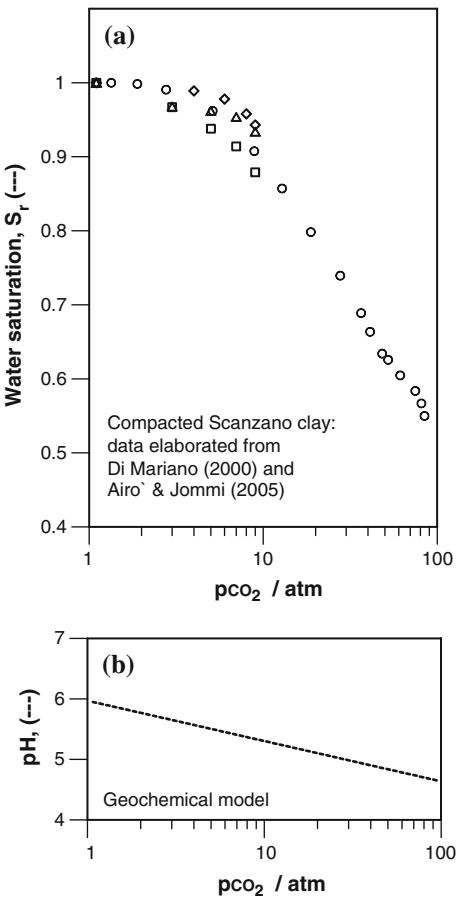

Fig. 9 Average final CO_2 pressure: (**a**) Representative capillary pressure curve of the treated soil; (**b**) corresponding pH value calculated with the geochemical model

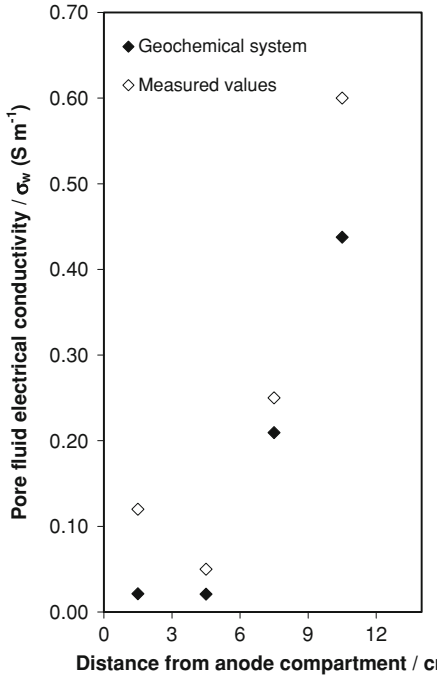

Fig. 10 Electrical conductivity of the pore fluid σ_w: measured and theoretical values calculated with the species considered in the geochemical system. Contributions from the non reactive species present in the interstitial pore fluid have not been taken into account in the theoretical calculations

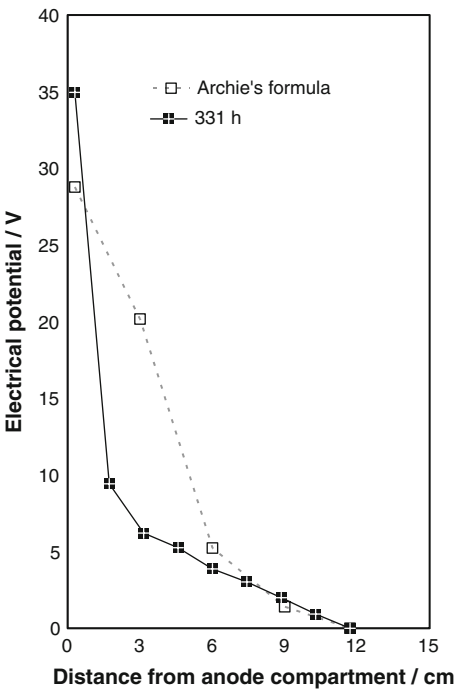

Fig. 11 Comparison between measured (*black symbols*) and calculated electrical potential after Archie's formula (*white symbols*). Figure refers to the end of Casp_er_01 test

calculated values are found to reproduce reasonably the experimental trend, although the conductivity in the first portion of the sample is overestimated. Since the microstructure of clay particle arrangements is influenced by the chemical composition of the pore fluid [9], tortuosity is changing as well. Introducing a dependency of the exponent *m* on the actual chemical conditions could enhance the prediciton of the model.

6 Conclusions

The experimental data presented in the paper highlight that the role of calcite, commonly found in natural soils, must be carefully evaluated when designing electrokinetic treatments. The geochemical model proposed for analysing the interaction between calcite and varying environmental conditions helps in explaining the buffering role of calcite and its consequent severe hydro-mechanical effects.

On the basis of the geochemical model presented, sharp change of pH, reduction of soil electrical conductivity, and development of persistent fractures close to the anode may be interpreted as consequences of arising severe CO_2 pressures in the anode area. Calcite dissolution and precipitation is held responsible for the changes of void ratio along the samples.

The model proposed was adopted to analyse the experimental data collected at test dismantling. The final activities of the species considered and CO_2 pressure were derived based on the measured final value of pH. In this way, the severe effects of CO_2 pressure developing during the treatment could be only partially analysed, and its role on fracture development and propagation could be only inferred from the experimental evidence.

Coupling of the geochemical model with an electro-hydro-mechanical transport model, that is under development, will enhance the possibility to analyse the evolution of the local constraint conditions imposed to the chemical system, and to model the transient response of the soil subjected to electrokinetic treatments.

Acknowledgments The financial support of the Italian Ministry of University and Research, through the project PRIN 2006080119-2006, *Experimental and theoretical study of the applicability of electrokinetic processes for the control of contaminant propagation in fine grained soils*, is gratefully acknowledged. The authors would like to thank Roberto Maniscalco for his kind support in the experimental activity at the Politecnico di Torino.

References

1. Corapcioglu MY (1991) Transp Porous Media 6:435
2. Alshawabkeh AN, Acar YB (1996) J Geotech Eng 122:186

3. Kim S, Kim JJ, Yun ST, Kim KW (2003) Water Air Soil Pollut 150:135
4. Mascia M, Palmas S, Polcaro AM, Vacca A, Muntoni A (2007) Electrochim Acta 52:3360
5. Al-Hamdan AZ, Reddy KR (2008) J Geotech Geoenviron Eng 134:91
6. Gajo A, Maines M (2007) Géotechnique 57:687
7. Chighini S, Lancellotta R, Musso G (2002) In: Vulliet L, Laloui L, Schrefler B (eds) Environmental geomechanics—Monte Verità 2002. EPFL Press, Lausanne, p 329
8. Virkutyte J, Sillanpää M, Latostenmaa P (2002) Sci Total Environ 289:97
9. Gabrieli L, Jommi C, Musso G, Romero E (2008) J Appl Electrochem 38:1043
10. ASTM (2005) D 4318: standard test methods for liquid limit, plastic limit and plasticity index of soils. ASTM Publication, Philadelphia
11. ASTM (2006) D 2487: standard practice for classification of soils for engineering purposes (unified soil classification system). ASTM Publication, Philadelphia
12. UNI (2004) 11140: determination of carbon dioxide. UNI, Milano
13. Musso G, Francia C, Maja M, Spinelli P (2002) Ann Chim 92:983
14. Appelo CAJ, Postma D (1993) Geochemistry, groundwater and pollution. Balkema, Rotterdam
15. Santamarina JC, Klein KA, Wang YH, Prencke E (2002) Can Geotech J 39:233
16. Mitchell JK, Soga K (2005) Fundamentals of soil behavior. Wiley, New York
17. Eykholt GR (1997) J Hazard Mater 55(1–3):171
18. Olivella S, Alonso EE (2008) Géotechnique 58:157
19. Di Mariano A (2000) PhD thesis, Università di Palermo
20. Airò Farulla C, Jommi C (2005) In: Bilsel H, Nalbantoglu Z (eds) Problematic soils, Geoprob 2005, vol 1, p 229
21. Iyer B (1990) In: Hoddinott KB, Lamb RO (eds) Physico-chemical aspects of soil and related materials. ASTM STP 1095, Philadelphia
22. Archie GE (1942) Trans AIME 146:54